

Validation of the analytical NSL for the Jupiter experiment

prepared by: F. Mignard
affiliation : OCA
approved by:
reference: GAIA-CA-TN-OCA-FM-037-2
issue: 2
revision: 0
date: 2012-04-05
status: Issued

Abstract

This note provides and validates an analytical version of the nominal scanning law meeting the accuracy requirement to search the best initial conditions for the Jupiter experiment. The analytical expressions are all compared to numerical integration to verify their accuracy and check that the free parameters are handled in the same way in both solutions. This validation is a necessary step to ensure that the optimal initial conditions have a perfectly understood meaning. This new release extends the versions released in March 2009 and January 2010 and corrects a serious shortcoming in the accuracy of the spin phase.

Document History

Issue	Revision	Date	Author	Comment
2	0	2012-04-04	FM	Deep revision of the solution for the spin phase in Sect.3.2 after discussions with L. Lindegren
1	4	2010-01-08	FM	Eqt. 26 expanded to order 10, for consistency with Eq. 27. Rev 4 issued to LL
1	3	2009-03-27	FM	Comments and typos provided by J. de Bruijne incorporated. Rev. 3 issued to LL
1	2	2009-03-24	FM	Improved the pdf for hyperlinks
1	1	2009-03-22	FM	First version issued
1	0	2009-03-04	FM	Creation

Contents

1 Introduction **4**

2 Equations of the NSL **5**

2.1 The Lindegren equation 7

2.2 Fundamental property of the solution 9

2.3 Analytical expression of the secular term 12

2.4 The free parameters 16

3 Solution of the differential equation **16**

3.1 The precession phase 16

3.1.1 Analytical solution 16

3.1.2 Comparison to numerical integration 20

3.2 The spin phase 25

3.2.1 The new solution 25

3.2.2 The analytical expression 25

3.2.3 Comparison to numerical integration 29

3.3 Implementation 31

4 Conclusion **31**

5 References **32**

1 Introduction

The on-going work aiming to optimise the scanning law for the Jupiter experiment is based on an intensive use of the analytical representation of the scanning law to find out the best values of the free parameters, namely the initial values of the precession angle and that of the spin at a prescribed time (J2010 in this work). Given the sensitivity of the science return of this experiment to the initial conditions, they must be searched with great care among all the possible values. This involves a large grid of exploration, typically every half-degree for the precession phase and every one or two degrees in the spin phase. The final output is very sensitive to the minute detail of the scanning because only a handful of efficient transits of Jupiter seen at small distance from a bright star contribute to the buildup of the relativistic signal.

The number of calls of the scanning law in this process is huge, since for every pair of initial conditions one must search all the possible transits of Jupiter over 5 years. From my own search software a full grid search amounts to $\sim 10^8$ calls of the scanning law. For each grid point one evaluates a merit function based on how well the light deflection by, e.g., the Jupiter quadrupole can be assessed with Gaia data. A typical diagram based on the standard analytical scanning law (the current version used for the simulation and implemented in the Gaia Tools and the values of the initial conditions are just indicative) is shown in Fig.1. Not surprisingly one sees that the optimisation is primarily driven by the choice of the precession initial value, while the selection of the initial spin phase looks more like a fine tuning.

However the final implementation of the scanning law will be based on the version to be delivered to the MOC by the DPAC in the form of a precomputed representation of the quaternions built upon a numerical integration and using the unique set of initial conditions determined during the optimisation search or from other mission constraints. Therefore it is important to demonstrate first that the analytical form and the numerical integration can agree to the required accuracy and that there is no problem to handle the free parameters in either representation. As far as the Jupiter experiment is concerned several values of the free parameters will be provided with respective factor of merit and new tests with the final scanning law should be conducted to validate the choice. Actually tests will be performed earlier by computing an ephemeris of the pointing directions, or that of the two scanning angles, with both versions using the same initial parameters.

In this note I primarily update and expand the accuracy of the analytical scanning law, since the needs are now more stringent than for simulation purposes, since we must predict real events on the sky. The new version is checked against numerical integration first to validate the accuracy and also to prove that initial conditions are defined in the same way in both cases.

In this second issue, the analytical solution of the spin phase has been fully revised to improve the accuracy and correct a mistake done in the comparison with the numerical integration which led to a claim of a spurious accuracy in the previous issue (0.015 deg instead of 0.2 deg in reality). The solution is now expanded to the 4th order of the small parameter and its accuracy

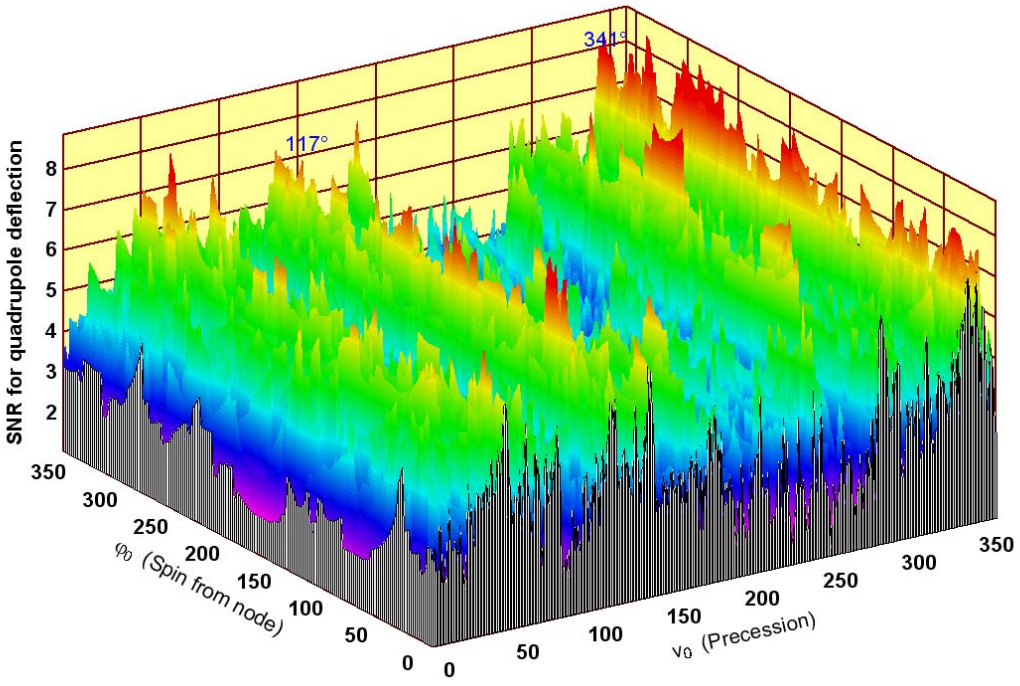


FIGURE 1: Example of a search for the best initial conditions of the scanning law for the detection of the light deflection by the quadrupole moment of Jupiter. The two horizontal axes run over $0 - 360$ degrees for the initial value of the precession angle and that of the spin phase. The merit function quantifies the level of detection of the relativistic deflection. The plot is based on a simple astrometric model without straylight. For more realistic features see REMAT presentations on-line.

compared to the exact numerical solution is 0.01 deg. Minor changes are also included in this note to document optimisations introduced over the last three years in the actual implementation both in Java and Fortran.

2 Equations of the NSL

The two differential equations defining the scanning law have been established in Lindegren (SAG-LL-014). These equations give the rate of change of the precession angle $v(t)$ and the spin angle $\Omega(t)$ shown in Fig. 2.

The precession angle $v(t)$ is solution of the differential equation,

$$\frac{dv}{dt} = \frac{1}{\sin\xi}\left((\dot{z}^2 - \dot{\lambda}^2\,\cos^2\,v)^{1/2} + \dot{\lambda}\cos\xi\,\sin v\right) \tag{1}$$

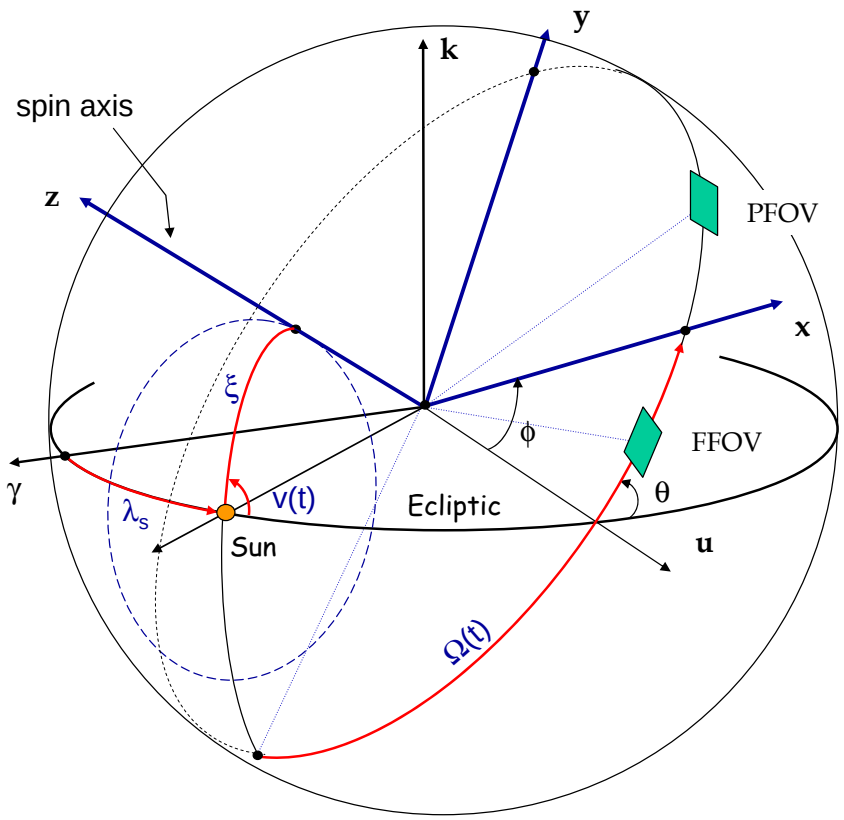


FIGURE 2: Geometric meaning of the parameters of the scanning law, with $v(t)$ for the precession and $\Omega(t)$ for the heliotropic spin phase. The diagram is drawn with $\xi < \pi/4$ for better clarity.

where λ is the sun longitude, ξ the sun-aspect angle set at 45 degrees for Gaia and $\dot{z}$ the instantaneous speed of the spin axis on the sky. Using the sun longitude as independent parameter instead of the time one gets,

$$\frac{dv}{d\lambda} = \frac{1}{\sin\xi}\left((S^2 - \cos^2 v)^{1/2} + \cos\xi \sin v\right) \tag{2}$$

where S is now a constant expressing the motion of the tip of the spin axis on the celestial sphere measured in solar longitude.

The equation for the spin phase has two forms according as it refers to the heliotropic angle (Lindegren (SAG-LL-014)) or to the Euler angle (Mignard (GAIA-FM-010)):

$$\frac{d\Omega}{dt} = \omega_z - \dot{\lambda}\sin\xi\sin v(t) - \dot{v}\cos\xi \tag{3}$$

for the heliotropic form and,

$$\frac{d\phi}{dt} = \omega_z - \dot{\lambda}\sin\xi\sin v(t) + \frac{\cos\xi\sin^2\xi\sin^2 v(t)}{1-\sin^2\xi\sin^2 v(t)}\,\dot{v} \tag{4}$$

for the Eulerian form.

Given the different origins to refer the spin phase, the two equations are in fact equivalent and either can be used, the transformation $\Omega \leftrightarrow \phi$ being a simple function of v and ξ with,

$$\begin{aligned} \cos(\Omega-\phi) &\propto -\cos v \\ \sin(\Omega-\phi) &\propto \quad \cos\xi\,\sin v \end{aligned} \tag{5}$$

where the proportionality factor is positive: $1/\sin(\theta)$ where θ is the inclination of the instantaneous scan circle to the ecliptic.

The spin-phase equation can be solved either from a quadrature once $v(t)$ is known, or in parallel by solving the two equations of a differential system.

The second form has been used in GAIA-FM-017 and the Fortran code provided also the quantity $\Omega(t) - \phi(t)$, allowing to change from one representation to the other. Although I initially worked with the Euler angle, I consider now preferable to do the optimisation search with the heliotropic angle to be closer to the DPAC usage and to avoid a potential source of confusion. In addition I overlooked in my earlier derivation of the analytical NSL that the equation for the spin phase can be solved in a more compact form and to a better approximation when the heliotropic representation is used (Sect. 3.2).

2.1 The Lindegren equation

As said earlier the optimisation for the relativity experiment is primarily concerned with the precession equation because of the sensitivity of the sky coverage to the phase of the precession angle. I refer to (2) now as the *Lindegren equation*, because he first derived this important equation for Gaia and also for its own sake. It provides a non-trivial example to study near periodic solutions with perturbation techniques, where perturbation series can be effectively worked out. This is a good example, not oversimplified, to illustrate a powerful mathematical method.

In this equation S is the precession speed constant, closely related to the velocity of the z-axis on the celestial sphere. It is constant when measured against the sun longitude and slightly variable when uniform time is used instead, the departure to uniformity being of the order of the solar orbit eccentricity, that is to say about $\pm 2\%$ of its average value. This effect was neglected

in the first version of the analytical scanning law currently implemented in the Gaiatools, with no harm for the simulations. This is obviously included in the updated version derived here used now for the preparation of the Jupiter experiment. As pointed out to me by L. Lindegren, neglecting the eccentricity generated an inconsistency since an eccentric orbit was used for the motion of the Sun, where the axis of the precession cone is kept pointing, while the time derivative of the precession axis on the sky was kept constant. This makes the loops slightly of variable size during the year.

In the RHS of (2) the dominant term is S which is of the order of $4-5$ (approximately the number of precession loops per year) in the case of Gaia. It determines the zero-order feature of the precession angle, namely a uniform revolution such that $dv/d\lambda \approx S$, telling that the precession speed is just $\sim S$ times faster than the sun on its orbit. The other terms in (2) are responsible for (i) the true precession speed being in fact $> S$ and (ii) the departure from a simple uniform motion. It is interesting to rewrite (2) as,

$$\frac{dv}{d\tau} = \left(1 - \frac{\cos^2 v}{S^2}\right)^{1/2} + \frac{\cos\xi \, \sin v}{S} \tag{6}$$

with

$$d\tau = \frac{S}{\sin\xi} \, d\lambda \tag{7}$$

This can also be rewritten formally as,

$$\frac{dv}{d\tau} = 1 + \psi(v) \tag{8}$$

where

$$\psi(v) = \left(1 - \frac{\cos^2 v}{S^2}\right)^{1/2} + \frac{\cos\xi \, \sin v}{S} - 1 \tag{9}$$

satisfying the fundamental properties,

$$\boxed{\begin{cases} \psi(v+2\pi) = \psi(v) & \\ \max_v |\psi(v)| < 1 & \text{if } S > 1 \end{cases}} \tag{10}$$

The second condition means that the precession rate $dv/d\tau$ has a constant sign. It is positive with the sign convention used implicitly above. The fact that this condition is true for $\psi(v)$ is

established by searching the max and min values with the roots of the first derivatives. There are two roots at $\pi/2, 3\pi/2$ if $S\cos\xi > 1$ and two more otherwise. In each case the extremes are less than one in absolute value.

Finally $1/S$ will be considered as the small parameter to expand the solution in a perturbative scheme to solve the equations to a certain order. Although $1/S$ appears in the close form of the equation, beyond the first order the expansion is in fact in powers of $1/S^2$. The form of the differential equation which is solved below is ,

$$\frac{dv}{d\tau} = 1 + \frac{\cos\xi\,\sin v}{S} - \frac{\cos^2 v}{2\,S^2} - \frac{\cos^4 v}{8\,S^4} + O(1/S^6) \tag{11}$$

The solution is searched up to $1/S^4$, although the secular term, linear in τ, is determined (from the exact differential equation) to $O((1/S^{10})$ for reasons to be explained later.

2.2 Fundamental property of the solution

It is shown now that the general solution of (8) satisfying (10) is the superposition of a linear secular term $\omega\tau$ and a periodic function with period $2\pi/\omega$. Therefore the solution will be searched in the form

$$v(\tau) = \omega\tau + \sum_k a_k\cos(k\,\omega\tau) + b_k\sin(k\,\omega\tau) \tag{12}$$

Proof. Consider the differential equation with more standard notations as,

$$\frac{dx}{dt} = 1 + \psi(x) \tag{13}$$

where conditions (10) are satisfied by $\psi(x)$. The solution in $t(x)$ can be written formally,

$$t(x) = \int_{x_0}^{x} \frac{du}{1+\psi(u)} \tag{14}$$

with $t(x_0) = 0$.

Now we have also,

$$t(x+2\pi) = \int_{x_0}^{x} \frac{du}{1+\psi(u)} + \int_{x}^{x+2\pi} \frac{du}{1+\psi(u)} \tag{15}$$

but with the periodicity condition on $\psi(x)$ the second integral over a range equal to a period does not depend on x and is a constant, T (provided the integral is defined, which is guaranteed by the second condition of (10)). This leads to the functional equation for $t(x)$

$$\forall x, \;\; t(x + 2\pi) - t(x) = T \tag{16}$$

meaning that $t(x)$ is fully defined by its restriction to the domain $[0,\, 2\pi[$. If we have two solutions of (16), $t_1(x)$ and $t_2(x)$, then $(t_2 - t_1)(x)$ is a solution of the homogeneous functional equation (without the RHS), whose solution is any periodic function $P(x)$ of period 2π. Therefore the general solution of (16) is the sum of the general solution of the homogenous solution and a particular solution of the inhomogeneous equation. Specifically the general solution can be written as,

$$\boxed{t(x) = \frac{T}{2\pi}\, x + P(x)} \tag{17}$$

that is to say a secular term in x and a periodic function of period 2π, which could be expanded in Fourier series.

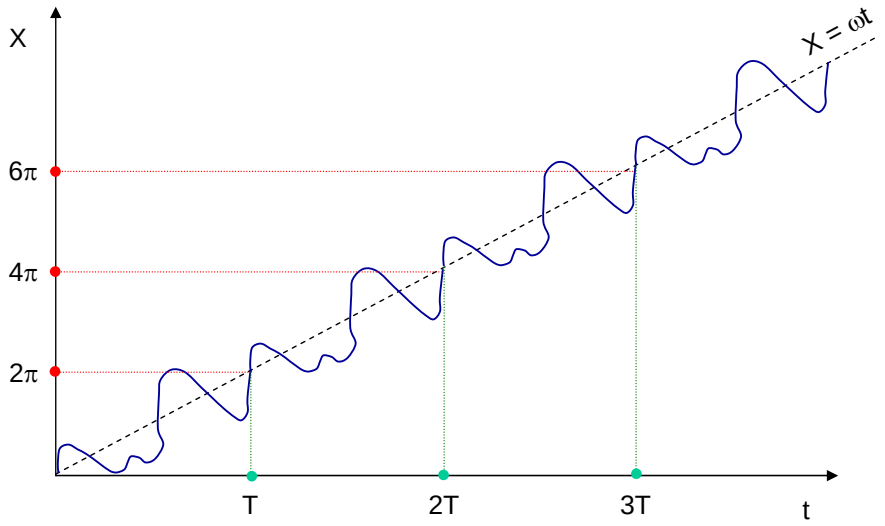


FIGURE 3: Qualitative representation of the periodic-secular pattern of the general solution of (13) showing the relationship between the T-step in the time domain and the 2π-step in the space domain. The plot is truly qualitative since with conditions (10), dX/dt is always positive and $X(t)$ is a one-to-one application.

This is not the end of the proof, since what is of interest here is the inverse function $x(t)$. But from the diagram,

$$\begin{array}{ccc} x & \longrightarrow & x+2\pi \\ \updownarrow & & \updownarrow \\ t & \longrightarrow & t+T \end{array}$$

it is clear that the functional equation (16) in the time domain has a counterpart in the space domain with the inverse function as,

$$\forall t, \;\; x(t+T) - x(t) = 2\pi \tag{18}$$

whose solutions is,

$$\boxed{x(t) = \frac{2\pi}{T}\, t + Q(t) = \omega\, t + Q(t)} \tag{19}$$

where $Q(t)$ is a periodic function of period T and $\omega = 2\pi/T$.

This concludes the proof that the general solution of the differential equation (13) with $\psi(x)$ satisfying (10) can be decomposed into a linearly secular term and a sum of periodic terms of period T or sub-multiples. It is slightly more than an existence theorem since we have also the period from the integral,

$$T = \int_0^{2\pi} \frac{du}{1+\psi(u)} \tag{20}$$

giving ω as $2\,\pi/T$ as,

$$\boxed{\omega = \frac{1}{\dfrac{1}{2\pi}\displaystyle\int_0^{2\pi} \frac{du}{1+\psi(u)}}} \tag{21}$$

which can be numerically evaluated. □

This result is general enough to deserve a second and totally different proof in the appendix based on properties of regular solutions of autonomous ordinary differential equations.

2.3 Analytical expression of the secular term

The integral (21) cannot be expressed in close form in the case of the scanning law, but either $\psi(v)$ is expanded before the integration in power of $1/S$, or a Taylor expansion of the integral is computed with a computer algebra software. This was my choice and most of the involved algebra was done with Maple.

When applied to Gaia with Eqs. 8-9 the evaluation of (21) yields the following after expansion to the 10th order in $1/S$:

$$\begin{aligned}\omega = 1 \\ &- \frac{1}{4\,S^2}\left(1+2\cos^2\xi\right) \\ &- \frac{1}{64\,S^4}\left(5-4\cos^2\xi+8\cos^4\xi\right) \\ &- \frac{1}{256\,S^6}\left(11-6\cos^2\xi-8\cos^4\xi+16\cos^6\xi\right) \\ &- \frac{1}{16384\,S^8}\left(469-232\cos^2\xi-176\cos^4\xi-320\cos^6\xi+640\cos^8\xi\right) \\ &- \frac{1}{65536\,S^{10}}\left(1379-658*\cos^2\xi-400*\cos^4\xi-416*\cos^6\xi-896*\cos^8\xi+1792*\cos^{10}\xi\right) \\ &+ O(1/S^{12})\end{aligned} \tag{22}$$

Using now (7) one can express this frequency with the solar longitude as independent variable as, (same notation as in SAG-LL-014).

$$K = \frac{S}{\sin\xi}\,\omega \tag{23}$$

that is to say,

$$
\begin{aligned}
K = & \frac{S}{\sin\xi}\left[1\right. \\
& - \frac{1}{4\,S^2}\left(1+2\cos^2\xi\right) \\
& - \frac{1}{64\,S^4}\left(5-4\cos^2\xi+8\cos^4\xi\right) \\
& - \frac{1}{256\,S^6}\left(11-6\cos^2\xi-8\cos^4\xi+16\cos^6\xi\right) \\
& - \frac{1}{16384\,S^8}\left(469-232\cos^2\xi-176\cos^4\xi-320\cos^6\xi+640\cos^8\xi\right) \\
& \left. - \frac{1}{65536\,S^{10}}\left(1379-658\cos^2\xi-400\cos^4\xi-416\cos^6\xi-896\cos^8\xi+1792\cos^{10}\xi\right)\right] \\
& + O(1/S^{12})
\end{aligned}
\tag{24}
$$

For $\xi = 45$ deg this reduces to the numerical expression,

$$
K = S\,\sqrt{(2)}\left(1-\frac{1}{2\,S^2}-\frac{5}{64\,S^4}-\frac{1}{32\,S^6}-\frac{309}{16384\,S^8}-\frac{898}{65536\,S^{10}}\right)+O(1/S^{12}) \tag{25}
$$

It is useful to have the reverse (i.e. inverse expanded to the same order) of this expansion to relate the number of precession periods per year (K) to the rate of motion of the spin axis on the sky (S) measured in mean solar motion. For practical purposes one may prefer to set the value of K, that is to say the number of revolutions per year instead of S, whereas the input parameter in the differential equation and the numerical integration is S. It is therefore important to have an accurate transformation between S and K for the cross-check between the analytical and numerical approaches. This again can be done with Maple and gives,

TABLE 2: For a sun aspect angle $\xi = 45$ deg, correspondence between the spin axis velocity S and the precession frequency K expressed in number of revolutions per year. The true values are derived from (21) and (23) with a numerical quadrature, while the approximation is evaluated with (24).

S	K(S) true	K(S) approx	S	K(S) true	K(S) approx
4.0	5.4783063552	5.4783063591	5.0	6.9287480784	6.9287480787
4.1	5.6241678862	5.6241678891	5.1	7.0729947618	7.0729947620
4.2	5.7698119090	5.7698119112	5.2	7.2171307914	7.2171307916
4.3	5.9152541653	5.9152541671	5.3	7.3611625802	7.3611625804
4.4	6.0605089008	6.0605089021	5.4	7.5050960522	7.5050960523
4.5	6.2055890400	6.2055890410	5.5	7.6489366883	7.6489366885
4.6	6.3505063370	6.3505063379	5.6	7.7926895677	7.7926895678
4.7	6.4952715066	6.4952715072	5.7	7.9363594036	7.9363594036
4.8	6.6398943367	6.6398943372	5.8	8.0799505760	8.0799505761
4.9	6.7843837877	6.7843837881	5.9	8.2234671611	8.2234671612

$$
\begin{aligned}
S = K\,\sin\xi * \Bigg[& 1 + \frac{1}{4\,K^2}\,\frac{1+2\cos^2\xi}{\sin^2\xi} \\
& + \frac{1}{64\,K^4}\,\frac{1-20\cos^2\xi-8\cos^4\xi}{\sin^4\xi} \\
& - \frac{1}{256\,K^6}\,\frac{1-18\cos^2\xi-88\cos^4\xi-16\cos^6\xi}{\sin^6\xi} \\
& - \frac{1}{16384\,K^8}\,\frac{7+8\cos^2\xi+4208\cos^4\xi+5952\cos^6\xi+640\cos^8\xi}{\sin^8\xi} \\
& + \frac{1}{65536\,K^{10}}\,\frac{11-130\cos^2\xi+6000\cos^4\xi+35168\cos^6\xi+24704\cos^8\xi+1792\cos^{10}\xi}{\sin^{10}\xi} \Bigg] \\
& + O(1/K^{12})
\end{aligned}
\tag{26}
$$

Again for $\xi = 45$ deg this reduces to the numerical expression,

TABLE 3: For a sun aspect angle $\xi = 45$ deg, correspondence between the precession frequency K and the rate of motion of the spin axis S, both expressed in number of revolutions per year. The numerical values follow from the expansion (27).

K	S(K)	K	S(K)	K	S(K)
5.0	3.6732774393	6.0	4.3583278215	7.0	5.0493860040
5.1	3.7414200308	6.1	4.4272086452	7.1	5.1187302370
5.2	3.8096544503	6.2	4.4961454994	7.2	5.1881109747
5.3	3.8779759680	6.3	4.5651358909	7.3	5.2575267915
5.4	3.9463801666	6.4	4.6341774699	7.4	5.3269763341
5.5	4.0148629159	6.5	4.7032680201	7.5	5.3964583171
5.6	4.0834203509	6.6	4.7724054492	7.6	5.4659715188
5.7	4.1520488509	6.7	4.8415877808	7.7	5.5355147775
5.8	4.2207450212	6.8	4.9108131466	7.8	5.6050869878
5.9	4.2895056756	6.9	4.9800797788	7.9	5.6746870972

$$S = \frac{K}{\sqrt{(2)}}\left(1 + \frac{1}{K^2} - \frac{11}{16\,K^4} + \frac{1}{K^6} - \frac{1847}{1024\,K^8} + \frac{3721}{1024\,K^{10}}\right) + O(1/K^{12}) \qquad (27)$$

A numerical check over a reasonable range of values of S and ξ has been performed showing that the two expressions are the inverse of each other to terms of the order of $1/S^{12}$. The differences between the input S in (24) to get K and the computed value from (26) are typically of the order of $0.2/S^{12}$ or about 6×10^{-9} with the Gaia parameters.

To give just one illustration, starting with $\xi = \pi/4$ and $S = 4.2$ in (24) yields

$$K = 5.76981191123564$$

and inserting this value in (26) returns

$$\tilde{S} = 4.20000002352647.$$

And also one has

$$S(5.769811876997) = 4.2.$$

If we aim at a consistency for the secular behaviour of 0.001 deg after 2000 days between the analytical and numerical solutions, one needs to have the transformations $K \leftrightarrow S$ to 5×10^{-7}. This is not difficult for $K(S)$ with a numerical quadrature, but more demanding for $S(K)$ since this amounts to solving an equation or performing an inverse interpolation with great accuracy. Table 3 gives the result to the required accuracy.

2.4 The free parameters

In addition to the initial condition $v_0(\tau_0)$, the Lindegren equation has two free parameters ξ and S. For Gaia, ξ is fixed once for all to $\pi/4$. The actual choice of S is in principle determined by the near overlapping condition proposed in SAG-LL-014 and expressed analytically to second order of $1/S^2$ in GAIA-FM-010. However this is more a general wish than something which can be given a perfect practical definition, as the time description of the loops does not reproduce strictly identically to each other. Furthermore, in a non-linear autonomous differential equation, the initial condition is not a simple additive parameter and the complete expression of the non-overlapping condition would depend on the initial condition. Above all, as shown by Lindegren, it is more important to satisfy approximately the non overlapping condition and use the remaining freedom to control the global loop pattern over the mission duration. Therefore in practice one knows that one must have something like,

$$S \approx \frac{3\pi}{2} \frac{\sin \xi}{\xi} \tag{28}$$

and then one selects K close to $K(S)$ such that there is an integral number of loops during the mission duration. For Gaia with $\xi = \pi/4$, this gives $S \approx 4.2$ and then $K = 5.6$ or 5.8. Then with (26) one obtains the corresponding value of S. This gives for the Gaia case, $S(5.6) = 4.0834203509$ and $S(5.8) = 4.2207450212$. The selected value of K is an input parameter for the analytical scanning law, while the corresponding value of S from (26) must be used for the function to be integrated. It appears now clearly why the expansion $S(K)$ and $K(S)$ had to be performed to a relatively high order to guarantee a perfect consistency between the analytical and numerical solutions. For Gaia the values of $K = 5.8$, giving approximately $S = 4.220$, has been chosen as the baseline by Astrium and impacts on several elements in the design and must be considered as a fixed reference. Only the two initial phases at a specified epoch remain free for the optimisation search.

3 Solution of the differential equation

3.1 The precession phase

3.1.1 Analytical solution

Equation (11) is solved by a perturbation method (the Poincaré-Lindstedt method), considering that the terms in $1/S, 1/S^2, \cdots$ are perturbations and that the solution can be uniformly approximated through an expansion in $1/S^k$. One takes also advantage of the decomposition of the solution into a secular term and a periodic function in $\omega\tau$. Rewriting the equation in the more

general form as before,

$$\frac{dx}{d\tau} = 1 + \psi(x) \tag{29}$$

where $\psi(x)$ is a small perturbation of first order. Then a solution is searched as

$$x(\tau) = x_0(\tau) + x_1(\tau) + x_2(\tau) + \dots \tag{30}$$

where $x_k(\tau)$ is of order k in the power of the small parameter. One must have also $x_0(\tau) = \omega\,\tau$ and $x_k(\tau),\ k > 0$ are periodic function in $\omega\,\tau$. Now using $\zeta = \omega\tau$ for the independent variable, the equation becomes,

$$\omega\,\frac{dx}{d\zeta} = 1 + \psi(x) \tag{31}$$

Expanding also ω in power of the small parameter as,

$$\omega = 1 + \omega_1 + \omega_2 + \dots \tag{32}$$

one can now plug (30) and (32) in (31) to write down the successive approximations.

For the first four orders this process leads to,

$$\begin{aligned}
\frac{dx_0}{d\zeta} &= 1 \\
\frac{dx_1}{d\zeta} + \omega_1\frac{dx_0}{d\zeta} &= \psi(x_0) \\
\frac{dx_2}{d\zeta} + \omega_2\frac{dx_0}{d\zeta} &= \psi'(x_0)\,x_1 - \omega_1\frac{dx_1}{d\zeta} \\
\frac{dx_3}{d\zeta} + \omega_3\frac{dx_0}{d\zeta} &= \psi'(x_0)\,x_2 + \frac{\psi''(x_0)}{2}\,x_1^2 - \omega_1\frac{dx_2}{d\zeta} - \omega_2\frac{dx_1}{d\zeta} \\
\frac{dx_4}{d\zeta} + \omega_4\frac{dx_0}{d\zeta} &= \psi'(x_0)\,x_3 + \psi''(x_0)x_1x_2 + \frac{\psi^{(3)}}{6}x_1^3 - \omega_1\frac{dx_3}{d\zeta} - \omega_2\frac{dx_2}{d\zeta} - \omega_3\frac{dx_1}{d\zeta} \\
&\vdots
\end{aligned} \tag{33}$$

At each step the right hand side is known from the solution of the lower orders and both the current x_k and ω_k are determined. In particular the ω_i are selected in such a way that only periodic terms are generated beyond the initial step. In addition I impose that the initial condition $x(0) = \alpha$ be such that $x_0(0) = x(0) = \alpha$ and then $x_k(0) = 0,\ k = 1, 2, \dots$.

When applied to the expansion of the Lindegren equation,

$$\frac{dv}{d\tau} = 1 + \frac{\cos\xi\,\sin v}{S} - \frac{\cos^2 v}{2\,S^2} - \frac{\cos^4 v}{8\,S^4} + O(1/S^6) \tag{34}$$

the whole process ends up with the analytical solution to the order $1/S^4$. With $\zeta = \omega\,\tau$ one has for the successive orders,

$$v_0 = \zeta + \alpha \tag{35}$$

$$v_1 = -\frac{1}{S}\,\cos\xi\,(\cos(\zeta+\alpha) - \cos(\alpha)) \tag{36}$$

$$\begin{aligned} v_2 = \frac{1}{S^2}\Big[& \frac{1}{2}\,\cos^2\xi\,\sin(\zeta) \\ & + \frac{1}{2}\,\cos^2\xi\,\sin(\zeta+2\alpha) \\ & - \frac{1}{8}\,(1+2\cos^2\xi)\,\sin(2\zeta+2\alpha) \\ & + \frac{1}{8}\,(1-2\cos^2\xi)\,\sin(2\alpha)\Big] \end{aligned} \tag{37}$$

$$\begin{aligned} v_3 = \frac{1}{S^3}\Big[& \frac{1}{16}\,\cos\xi\,\cos(\zeta-\alpha) \\ & + \frac{1}{16}\,\cos\xi\,\cos(\zeta+\alpha) \\ & - \frac{1}{16}\,(\cos\xi - 4\cos^3\xi)\,\cos(\zeta+3\alpha) \\ & - \frac{1}{8}\,(\cos\xi + 2\cos^3\xi)\,\cos(2\zeta+\alpha) \\ & - \frac{1}{8}\,(\cos\xi + 2\cos^3\xi)\,\cos(2\zeta+3\alpha) \\ & + \frac{1}{48}\,(5\cos\xi + 4\cos^3\xi)\,\cos(3\zeta+3\alpha) \\ & + \frac{1}{4}\cos^3\xi\cos\alpha + \frac{1}{12}(\cos\xi - \cos^3\xi)\,\cos 3\alpha\Big] \end{aligned} \tag{38}$$

$$
\begin{aligned}
v_4 = \frac{1}{S^4}\Big[& -\frac{1}{16}\,(\cos^2\xi - 4\cos^4\xi)\,\sin(\zeta) \\
& + \frac{1}{96}\,\cos^2\xi\,\sin(\zeta - 2\alpha) \\
& + \frac{1}{8}\,\cos^4\xi\,\sin(\zeta + 2\alpha) \\
& + \frac{1}{96}\,(7\cos^2\xi - 12\cos^4\xi)\,\sin(\zeta + 4\alpha) \\
& + \frac{1}{64}\,(1 + 4\cos^2\xi + 4\cos^4\xi)\,\sin(2\zeta) \\
& - \frac{1}{48}\,(3 - 8\cos^2\xi - 6\cos^4\xi)\,\sin(2\zeta + 2\alpha) \\
& - \frac{1}{64}\,(1 - 4\cos^2\xi - 12\cos^4\xi)\,\sin(2\zeta + 4\alpha) \\
& - \frac{1}{32}\,(5\cos^2\xi + 4\cos^4\xi)\,\sin(3\zeta + 2\alpha) \\
& - \frac{1}{32}\,(5\cos^2\xi + 4\cos^4\xi)\,\sin(3\zeta + 4\alpha) \\
& + \frac{1}{768}\,(3 + 52\cos^2\xi + 24\cos^4\xi)\,\sin(4\zeta + 4\alpha) \\
& + \frac{1}{16}\,(1 - 2\cos^4\xi)\,\sin(2\alpha) + \frac{1}{256}\,(3 - 12\cos^2\xi + 8\cos^4\xi)\,\sin(4\alpha)\Big]
\end{aligned}
\tag{39}
$$

This seems a bit impressive, but all the coefficients can be reduced to numbers or even to irreducible fractions when $\xi = \pi/4$, and the total number of terms is not very large.

Remark I: One must notice that the initial precession phase α appears in a non-linear way in many trigonometric lines and that the general solution $v(\tau, \alpha)$ with initial condition α, cannot be deduced (at least in a practical way) from $v(\tau, 0)$. The full solution $v(\tau, \alpha)$ must be implemented to search for the optimal value of α. Stated in another way, while $\tilde{v}(\tau, \alpha) = v(\tau, 0) + \alpha$ takes the correct value α at $\tau = 0$, it is not a solution of the differential equation and cannot be used to generate the general solution from $v(\tau, 0)$. The only general property which can be stated regarding the change of origin of time, is that if there is a solution $\tau^\star$ to the equation,

$$v(\tau, 0) = \alpha \tag{40}$$

then $v(\tau, \alpha) = v(\tau + \tau^\star, 0)$. This is true because the differential equation is autonomous and invariant by translation in the origin of time. But solving (40) to the required accuracy is much more demanding than using directly $v(\tau, \alpha)$.

Remark II: Since the ω_k are determined at the same time as the x_k, one could have derived the expression of ω given in (22) through the successive approximations. However to get the expansion to 8th order in $1/S$ one would have had to reach this level of approximation in the

successive approximations, a really daunting task and a waste of effort since we don't need the periodic terms to that accuracy. Therefore having a shortcut to evaluate ω proves very useful. At least to the 4th order, I have checked that the two methods agree.

3.1.2 Comparison to numerical integration

The full precession equation has been integrated with a Bulirsch and Stoer algorithm, after a preliminary validation with two other built-in codes from Maple and Matlab. The numerical precision checked by a close-path integration. The analytical solution was implemented in a Fortran code (see Sect. 3.3). Different values of the initial condition α were tested and in each test the same value was used as input for the numerical and analytical solutions. A value of $K = 5.8$ revolution per year was used in the analytical solution and $S = 4.2207450$ (Table 3) in the differential equation. Nominally the solution was integrated over 2000 days and different time steps were used for validation purposes. To test the lack of a secular trend, special integrations have been performed over $20,000$ and even $100,000$ days and no trend was detected with the above pair of K, S. A trend becomes noticeable by just changing the last digit of a few units.

Results are shown in a set of plots in Figs. 4-7 as higher order terms are entered in the analytical solution. For each plot giving the difference between the two methods, I also include a Fourier transform of this difference. The magnitude of the residuals is in good agreement with the values expected for a given order. In each spectrum one recovers at each step the leading terms of the next order in the analytical solution.

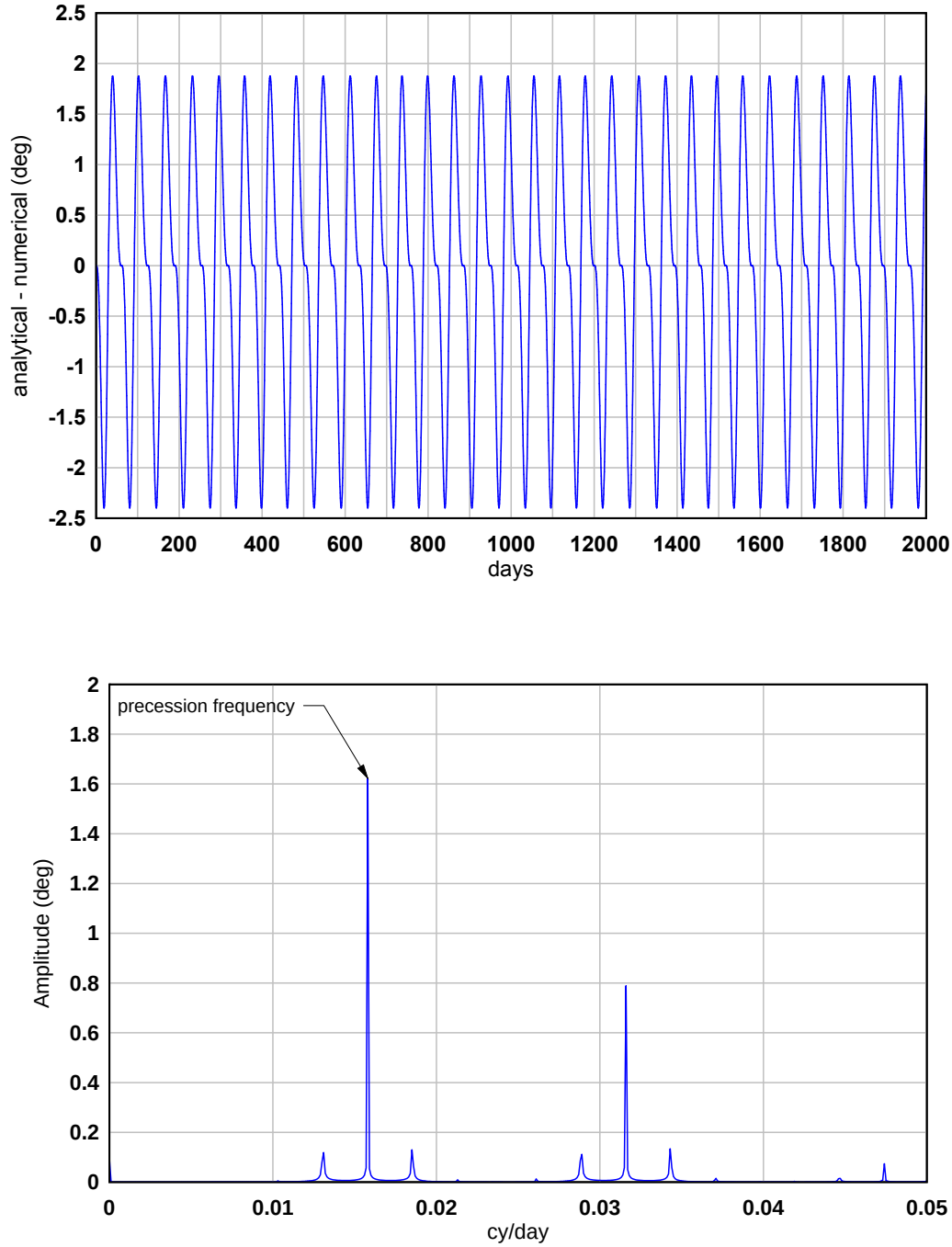


FIGURE 4: Difference between the first order analytical solution and the numerical integration over 2000 days (top) and its Fourier spectrum (bottom). The precession frequency corresponds to a period of about 64 days. The difference between the main harmonics and the satellite lines is 0.00273 cy/day, that is to say a one-year period.

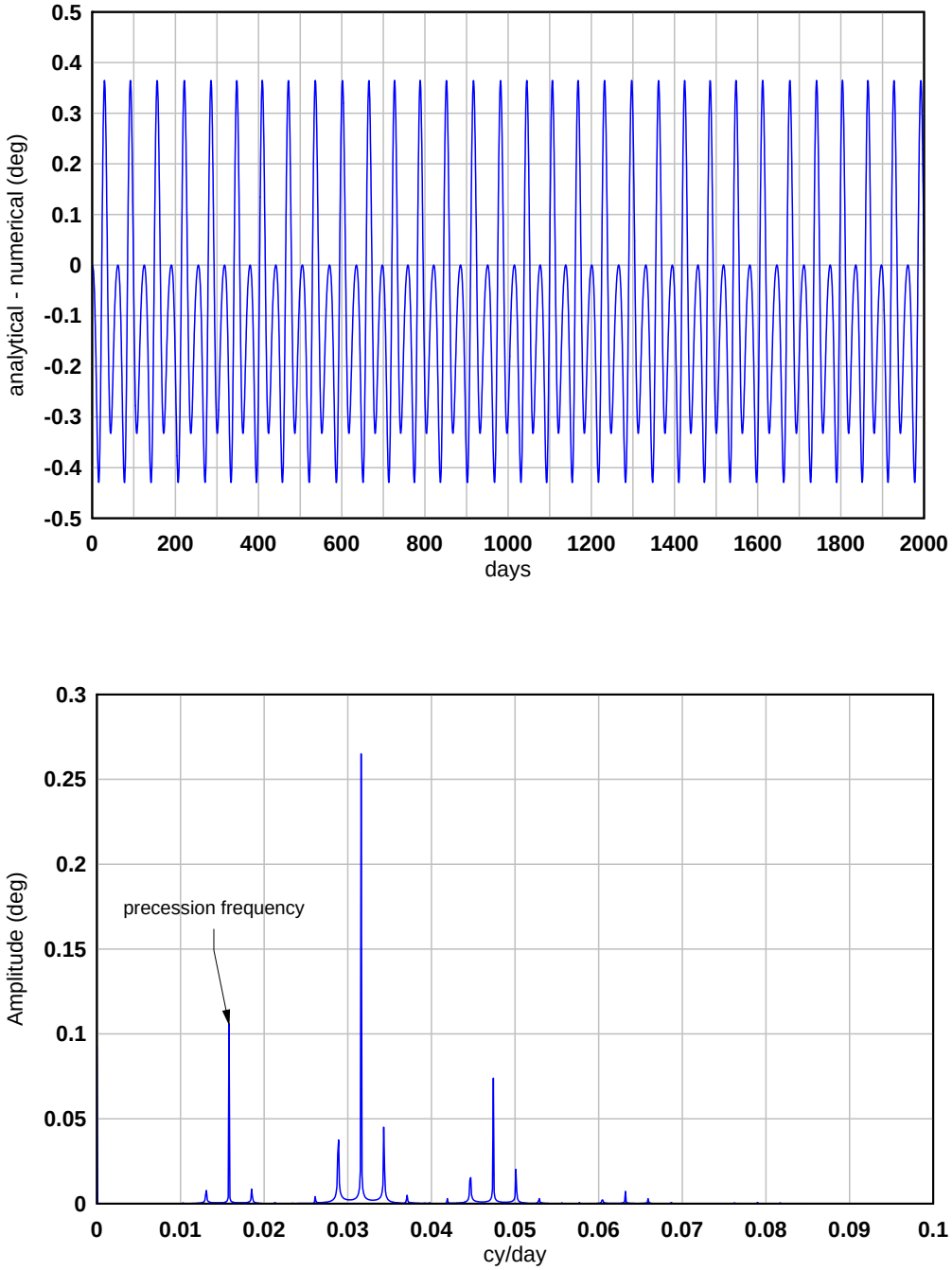


FIGURE 5: Difference between the second order analytical solution and the numerical integration over 2000 days (top) and its Fourier spectrum (bottom). The precession frequency corresponds to a period of about 64 days. The difference between the main harmonics and the satellite lines is 0.00273 cy/day, that is to say a one-year period.

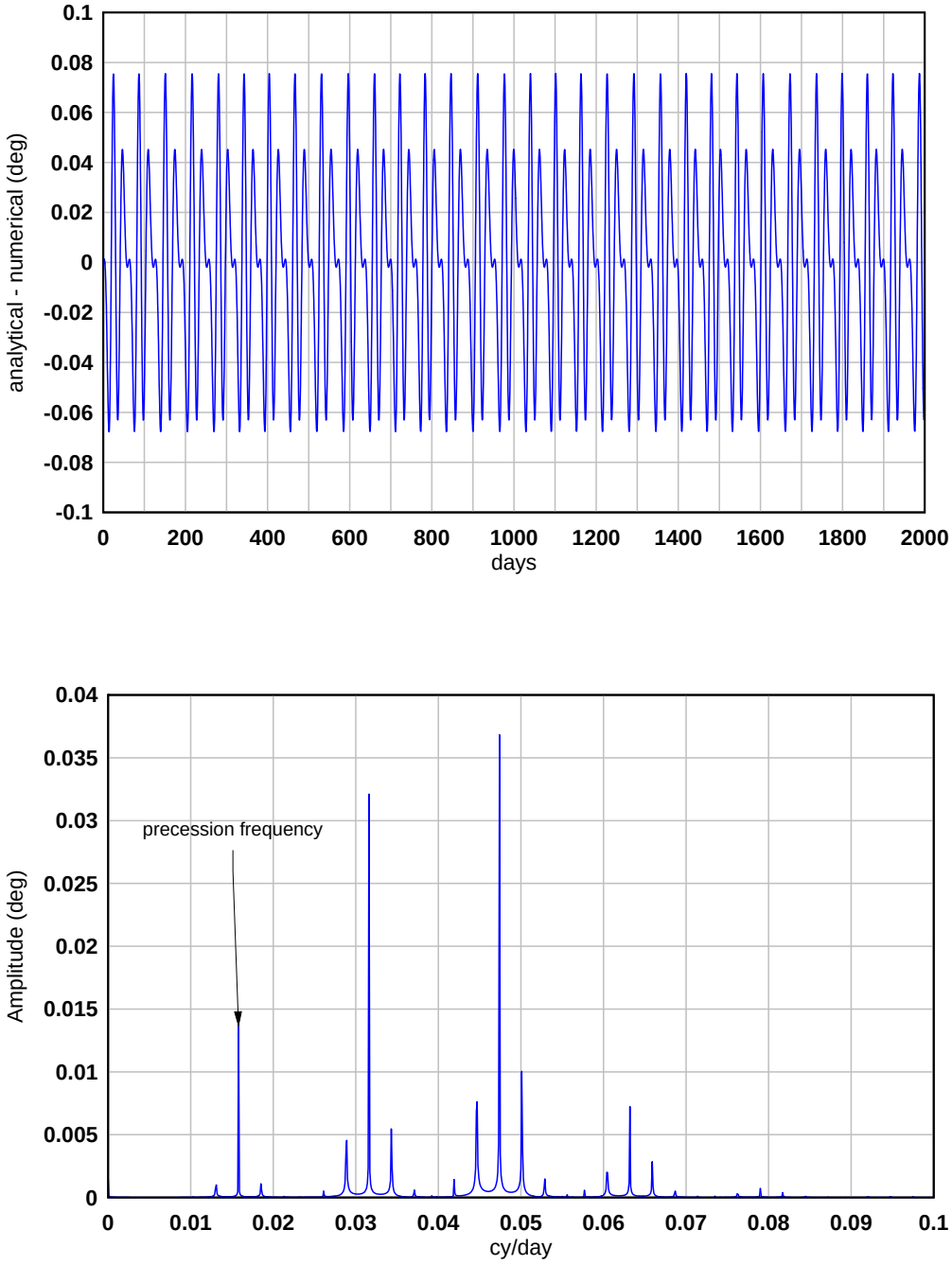


FIGURE 6: Difference between the third order analytical solution and the numerical integration over 2000 days (top) and its Fourier spectrum (bottom). The precession frequency corresponds to a period of about 64 days. The difference between the main harmonics and the satellite lines is 0.00273 cy/day, that is to say a one-year period.

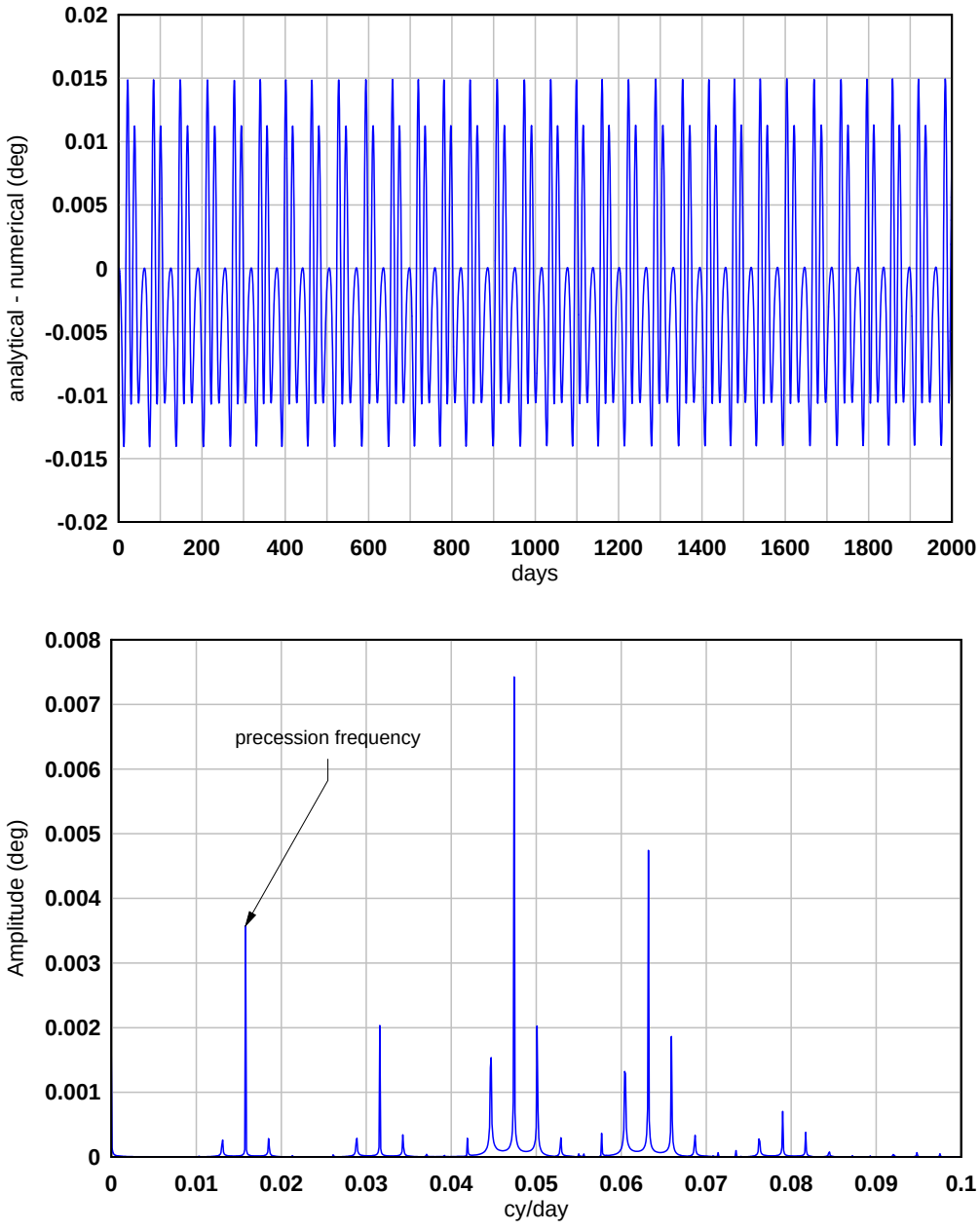


FIGURE 7: Difference between the fourth order analytical solution and the numerical integration over 2000 days (top) and its Fourier spectrum (bottom). The precession frequency corresponds to a period of about 64 days. The difference between the main harmonics and the satellite lines is 0.00273 cy/day, that is to say a one-year period.

3.2 The spin phase

3.2.1 The new solution

In this second issue of the note, this section on the spin phase has been partially rewritten to include changes implemented in the computer versions in 2011 (both in Fortran and Java) and not documented in an updated version of the Technical Note. Moreover a discussion with L. Lindegren in March 2012 has led to the discovery that the comparison to the numerical integration presented in the note was too optimistic. This was fully related to the bug spotted in March 2011, without realising at that time that this invalidated also the analysis presented in the technical note. The residuals found and shown in the first release of this note were below 0.015 degree while they were in fact of the order of 0.2 degree. This small, but erroneous, residual determined where I stopped the expansion in power of the small parameter and naturally this was done at the wrong level. This is corrected in this version of the note, which is now in agreement with the implemented code.

3.2.2 The analytical expression

This case is much simpler than for the precession equation since it reduces to a quadrature of a known function of time. The initial condition Ω_0 is purely additive and unlike the precession angle, raises no special problem. Thus the general solution is simply,

$$\Omega(t, \Omega_0) = \Omega_0 + \Omega(t, 0) \tag{41}$$

I have adopted the heliotropic origin instead of the node between the ecliptic and the scanning plane to conform with the practice in the implementation of the scanning law in the Gaia tool, although this choice has no definite advantage. The analytical solution is essentially taken from GAIA-FM-017, except for the solution of the term in $\dot{v}$ in (3) whose solution is directly given by $\cos\xi\,[v(t) - v(0)]$.

Rewriting (3),

$$\frac{d\Omega}{dt} = \omega_z - \dot{v}\cos\xi - \dot{\lambda}\sin\xi\sin v(t), \tag{42}$$

one sees that the integration of the first and second term of the RHS is trivial. For the last term, while the integral is nominally over the time, it is easier to use the precession angle $v(t)$ as independent variable with (2) and evaluate,

$$\delta\Omega(v) = -\int_{v(0)}^{v(t)} \frac{\sin^2\xi\sin v}{(S^2 - \cos^2 v)^{1/2} + \cos\xi\,\sin v}\,dv \tag{43}$$

As earlier $\delta\Omega(v)$ expressed as a function of $v(t)$ comprises a secular term linear in v and a periodic part with period 2π as illustrated in Fig. 8.

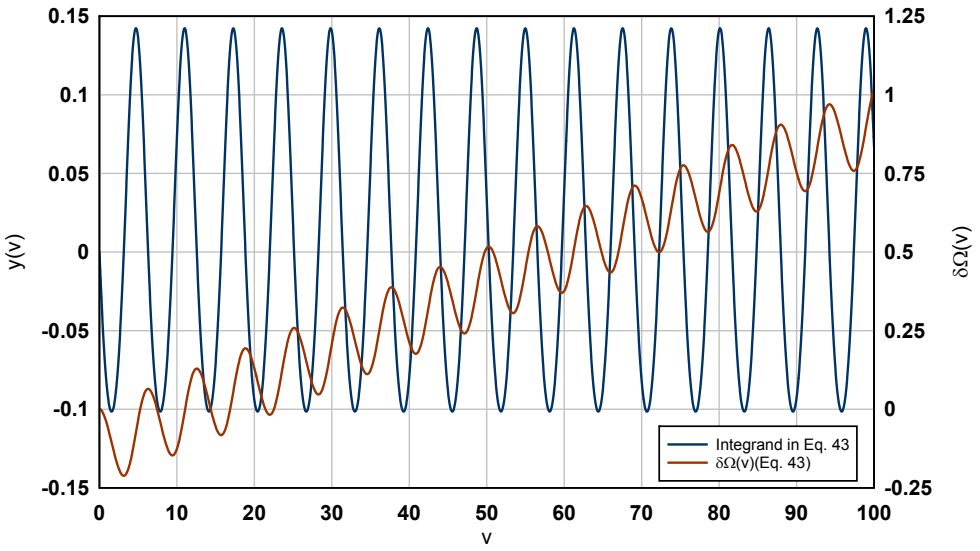


FIGURE 8: Plot of the integrand in Eq. 43 (including the minus sign) and of the integral (43) over $v = 0..100$ radians. The average of the integrand is slightly positive and the slope found of 0.01/radian is in full agreement with the first term of the secular drift in $v(t)$ in Eq. 51, $\sim \sin^2\xi\cos\xi/2S^2$. Gaia values have been used with $S = 4.22$ and $\xi = 45$ deg.

This solution will take the form,

$$\delta\Omega(v) = a_0(v - v_0) + \sum_{k=1}^{k=\infty} a_k\left[\cos kv(t) - \cos kv(0)\right] + b_k\left[\sin kv(t) - \sin kv(0)\right] \tag{44}$$

where the coefficients a_k, b_k are easily related to the Fourier expansion of the integrand,

$$\mathcal{I}(v) = \frac{\sin^2\xi\sin v}{(S^2 - \cos^2 v)^{1/2} + \cos\xi\,\sin v} \tag{45}$$

written as,

$$\tilde{a}_0 + \sum_{k=1}^{k=\infty} \tilde{a}_k\,\cos kv(t) + \tilde{b}_k\,\sin kv(t) \tag{46}$$

giving by integration of Eq. 46 (or derivation of Eq. 44),

$$\begin{aligned} a_0 &= \tilde{a}_0 \\ a_k &= -\tilde{b}_k/k \\ b_k &= \tilde{a}_k/k \end{aligned} \tag{47}$$

With a computer algebra software one can expand the integrand in power of $1/S$ and perform the Fourier expansion with formal algebra to obtain the $\tilde{a}_k, \tilde{b}_k$ in power of $1/S$.

The $\tilde{a}_k, \tilde{b}_k$ are then computed from,

$$\tilde{a}_0 = \frac{1}{2\pi}\int_0^{2\pi} \mathcal{I}(v)\, dv \tag{48}$$

$$\tilde{a}_k = \frac{1}{\pi}\int_0^{2\pi} \mathcal{I}(v)\cos(kv)\, dv, \qquad k > 0 \tag{49}$$

$$\tilde{b}_k = \frac{1}{\pi}\int_0^{2\pi} \mathcal{I}(v)\sin(kv)\, dv, \qquad k > 0 \tag{50}$$

The contribution to the secular term directly proportional to $v(t)$ has been expressed to $1/S^8$ to secure a better accuracy on the mean rate. The other contributions are given to 5th order so that the periodic residuals with respect to a numerical integration are less than 0.01 degree. In practice the final residual is dominated by the term in zero order in $v(t)$, which propagates directly into the spin phase (damped by a factor $\cos\xi \sim 0.7$). Since the analytical representation of $v(t)$ is accurate to ~ 0.015 deg, one cannot expect the final accuracy in $\Omega(t)$ better than 0.01 deg for the periodic terms. I stopped the expansion to 5th order in agreement with this fact. However, similarly as for the precession, the mean rate must be better represented and the expansion is carried out to order 8.

After some programming on Maple one gets to the required approximation,

$$
\begin{aligned}
\Omega(t) &= \Omega_0 + \omega_z(t-t_0) \\
&- \cos\xi\,[v(t)-v(0)] \\
&+ \sin^2\xi\cos\xi \\
&\quad \left[\frac{1}{2\,S^2} + \frac{1+3\cos^2\xi}{8\,S^4}\right. \\
&\quad + \frac{1+2\cos^2\xi+5\cos^4\xi}{16\,S^6} \\
&\quad \left. + \frac{5+9\cos^2\xi+15\cos^4\xi+35\cos^6\xi}{128\,S^8}\right][v(t)-v(0)] \\
&+ \sin^2\xi\left[\frac{1}{S} + \frac{1+6\cos^2\xi}{8\,S^3} + \frac{3+12\cos^2\xi+40\cos^4\xi}{64\,S^5}\right][\cos\,v(t) - \cos\,v(0)] \\
&- \sin^2\xi\,\cos\xi\left[\frac{1}{4S^2} + \frac{\cos^2\xi}{4S^4}\right][\sin 2v(t) - \sin 2v(0)] \\
&+ \sin^2\xi\left[\frac{1-2\cos^2\xi}{24\,S^3} + \frac{9+12\cos^2\xi-40\cos^4\xi}{384\,S^5}\right][\cos\,3v(t) - \cos\,3v(0)] \\
&- \sin^2\xi\,\cos\xi\left[\frac{1-\cos^2\xi}{32\,S^4}\right][\sin\,4v(t) - \sin\,4v(0)] \\
&+ \sin^2\xi\left[\frac{3-12\cos^2\xi+8\cos^4\xi}{640\,S^5}\right][\cos\,5v(t) - \cos\,5v(0)] \\
&+ O(1/S^6)
\end{aligned}
\tag{51}
$$

For the purpose of implementation the part coming from Eq. 43, can be ordered in power of $1/S$ as,

$$
\begin{aligned}
\frac{\delta\Omega(t)}{\sin^2\xi} &= \frac{1}{S}\left[\cos\, v(t) - \cos\, v(0)\right] \\
&- \frac{1}{S^2}\frac{\cos\xi}{4}\left[\sin 2v(t) - \sin 2v(0)\right] \\
&+ \frac{1}{S^3}\left[\frac{1+6\cos^2\xi}{8}\left[\cos\, v(t) - \cos\, v(0)\right] + \frac{1-2\cos^2\xi}{24}\left[\cos\, 3v(t) - \cos\, 3v(0)\right]\right] \\
&- \frac{1}{S^4}\left[\frac{\cos^3\xi}{4}\left[\sin 2v(t) - \sin 2v(0)\right] + \left[\frac{\cos\xi - \cos^3\xi}{32}\right]\left[\sin\, 4v(t) - \sin\, 4v(0)\right]\right] \\
&+ \frac{1}{S^5} \\
&\quad \left\{\left[\frac{3+12\cos^2\xi+40\cos^4\xi}{64}\right]\left[\cos\, v(t) - \cos\, v(0)\right]\right. \\
&\quad + \left[\frac{9+12\cos^2\xi-40\cos^4\xi}{384}\right]\left[\cos\, 3v(t) - \cos\, 3v(0)\right] \\
&\quad \left. + \left[\frac{3-12\cos^2\xi+8\cos^4\xi}{640}\right]\left[\cos\, 5v(t) - \cos\, 5v(0)\right]\right\} \\
&+ O(1/S^6)
\end{aligned}
\tag{52}
$$

3.2.3 Comparison to numerical integration

The comparison with the full integration is shown in Fig. 9. Due to the limited accuracy on the secular term (terms in $1/S^{10}$ neglected) I took for the plots $\omega_z = 60.0000000175$ deg/hour as input of the analytical formula while using $\omega_z = 60$ deg/hour in the numerical integration, to get a perfect fit over the long term. Keeping 60 deg/hour instead yields a drift of 0.0008 degree after 2000 days between the two solutions. Even without correction, this would not invalidate the conclusions of the optimisation search, just changing the crossing date by 0.1 seconds, corresponding to a displacement of Jupiter relative to the stars of ~ 1 mas. Using the earlier formulation with the Eulerian form and adding the heliotropic abscissa of the node to the spin phase (Eq. 5) produces the same results at this level of approximation.

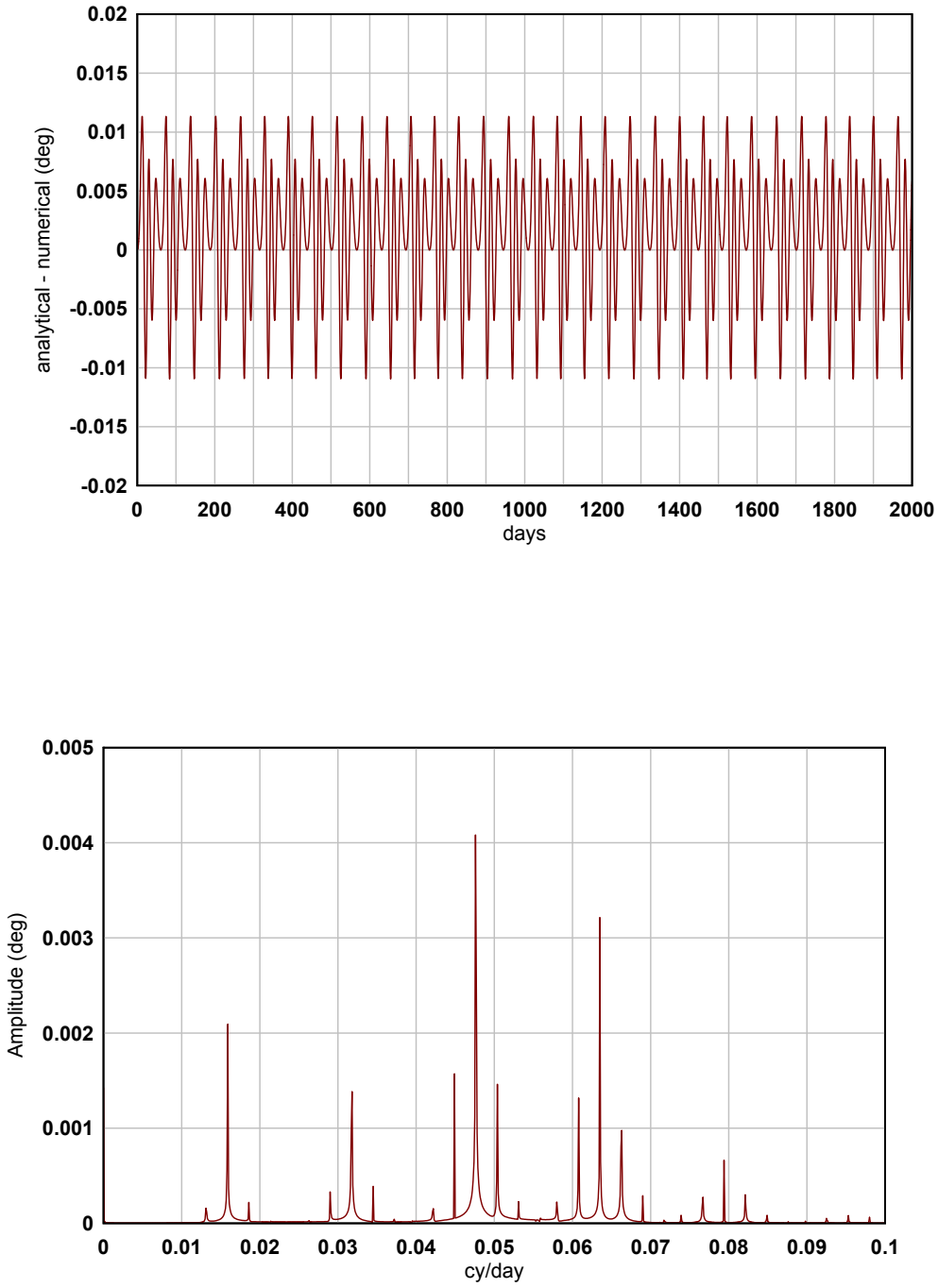


FIGURE 9: Difference for the spin phase $\Omega(t)$ between the analytical solution and a numerical integration over 2000 days (top) and its Fourier spectrum (bottom). The signatures in the Fourier domain depends only on combinations of the precession frequency with the solar motion.

3.3 Implementation

The algebra of the analytic solution may appear at first glance not very efficient to be written down in a Fortran or Java program. Actually, even by keeping the sun-aspect angle as a free parameter, all the coefficients depending on $\cos(\xi), \sin(\xi)$ can be evaluated once for all in a program, taking advantage of the static variable (with the attribute *save* in Fortran). Then the multiples of trigonometric lines like $\cos(k\zeta), \cos(k\alpha)$ are quickly evaluated with a recurrence relation. Finally the combinations $\cos(i\zeta + j\alpha)$ are expanded and computed with two products and one sum. In practice the program is very fast and on my desktop computer it takes 3s for 10^6 calls, with the optimised routine. Just to compare with numerical integration, in the most favourable case where one builds an ephemeris, where the successive calls advance the time just from one little step, (i.e. $1/10^6$ the total range of the ephemeris) the execution time is five times larger. But this does not correspond to the more demanding situation in a simulation where the scanning must be computed from scratch to any time in the interval of 2000 days. Finally, the execution time is not really the issue as factor five could be overcome with a good organisation of the computation. For testing a grid of initial conditions, a simple and self-contained subroutine remains much easier to use.

4 Conclusion

In this note I have provided:

- an enhanced version of the analytical scanning law accurate to 0.01 deg relative to an exact numerical integration both in precession and spin phase;
- a fully accurate representation of the secular trend of the solution to better than 0.001 deg over 2000 days;
- a general mathematical result regarding the overall pattern of solutions of a particular category of first order ordinary differential equations.

The corresponding Fortran code has the same interface as the earlier version and has been plugged into the Solar system transit simulator to determine Jupiter transits for different initial conditions. This was a prerequisite before one can work out the optimisation search on a bigger scale and see how this fits in with the Gaia scanning law (including the MSL).

Acknowledgements

Stimulating discussions with Michel Hénon and Fathi Namouni from the Laboratory Cassiopée in Nice proved very useful in the formulation of the overall properties of the general solution

presented in Sect. (2.2. Thanks are also due to Lennart Lindegren who pointed out a problem with the accuracy of the spin phase in an earlier version of this note.

5 References

[SAG-LL-014], Lindegren, L., 1998, *The scanning law for GAIA.*,
SAG-LL-014,
URL http://www.rssd.esa.int/llink/livelink/open/357121

[GAIA-FM-010], Mignard, F., 2001, *A practical scanning law for GAIA simulations*,
GAIA-FM-010,
URL http://www.rssd.esa.int/llink/livelink/open/358637

[GAIA-FM-017], Mignard, F., 2004, *The practical scanning law - an update*,
GAIA-FM-017,
URL http://www.rssd.esa.int/llink/livelink/open/356876

Appendix

In this appendix I provide an independent derivation of the fundamental rate ω in the solution of the differential equation,

$$\frac{dx}{dt} = 1 + \psi(x) \tag{53}$$

where as before $\psi(x)$ satisfies the two conditions (10). For a solution having the form

$$x(t) = \omega\, t + P(t) \tag{54}$$

where $P(t)$ is a periodic function of period $2\pi/\omega$, with

$$\forall t, \qquad |P(t)| < \infty. \tag{55}$$

Here ω is the mean rate of growth of $x(t)$ and one has

$$\omega = \langle \frac{dx}{dt} \rangle = 1 + \langle \psi(x) \rangle \tag{56}$$

where the operator $\langle f \rangle$ stands for the time average of $f(t)$.

For the perturbation term $\psi(x)$, the average along an integral curve of (53) can be written as,

$$\langle \psi(x(t)) \rangle = \lim_{T\to\infty} \frac{1}{T} \int_0^T \psi(x) dt \tag{57}$$

and by turning the integration over t into one over x,

$$\langle \psi(x(t)) \rangle = \lim_{T\to\infty} \frac{1}{T} \int_{x_0}^{x(T)} \frac{\psi(x)}{dx/dt} dx = \lim_{T\to\infty} \frac{1}{T} \int_{x_0}^{x(T)} \frac{\psi(x)}{1+\psi(x)}\, dx \tag{58}$$

which amounts to changing a time average into a space average. But we know that $\psi(x) = \psi(x + 2\pi)$, and the integral over a long interval of x can be replaced by the sum of the number of times this interval contains 2π (it is easy to show that the remainder above an integral number of 2π is bounded and becomes negligibly small when divided by T and $\to 0$ as $T \to \infty$) . Therefore (56) can then be rewritten,

$$\langle \frac{dx}{dt} \rangle = \lim_{T\to\infty} \frac{1}{T} \frac{x(T)}{2\pi} \int_0^{2\pi} \frac{\psi(x)}{1+\psi(x)}\, dx \tag{59}$$

But with (54) and (55) we have also

$$\lim_{T\to\infty} \frac{x(T)}{T} = \omega \tag{60}$$

and with a straight substitution in (59), one can resolve for ω and gets,

$$\boxed{\omega = \frac{1}{\dfrac{1}{2\pi}\displaystyle\int_0^{2\pi} \frac{dx}{1+\psi(x)}}} \tag{61}$$

a result identical to (20) but based on very different considerations. One should notice that this establishes only what the period should be, provided that (54) is true. This latter fact has been proved in Sect.2.2.